crystals

MDPI

Article

Effect of Phase Composition Variation of Oxy–Nitride Composite Ceramics on Heat Resistance and Preservation of Strength Parameters

Daryn B. Borgekov [1,2,*], Serik B. Azambayev [1], Artem L. Kozlovskiy [1] and Dmitriy I. Shlimas [1,2]

[1] Engineering Profile Laboratory, L.N. Gumilyov Eurasian National University, Astana 010008, Kazakhstan; mr.azambaev@mail.ru (S.B.A.); shlimas@inp.kz (D.I.S.)
[2] Laboratory of Solid State Physics, Institute of Nuclear Physics, Almaty 050032, Kazakhstan
* Correspondence: d.borgekov@inp.kz; Tel./Fax: +77-024413368

Abstract: The aim of this study is to determine the effect of changes in the phase composition of Al_2O_3–Si_3N_4 ceramics that were obtained using the method of mechanochemical solid-phase grinding on their resistance to the process of long-term thermal exposure, accompanied by the processes of oxidation and softening. The relevance of this research consists of determining the influence of the phase composition of ceramics on the change in their strength and thermophysical parameters, on the basis of which, we can draw a conclusion about the optimal composition of composite ceramics that have great prospects in the field of fire-resistant, heat-resistant, or radiation-resistant structural materials. During this study, the dynamics of the changes in the phase transformations of the xAl_2O_3–$(1-x)Si_3N_4$ ceramics, with variations in the ratio of the components, initiated by the thermal annealing of the samples, was established. According to the assessment of the phase transformations with variations in the ratio of the components, it was found that thermal annealing in an air environment at an Al_2O_3 concentration in the order of 0.3–0.5 M leads to the formation of an orthorhombic $Al_2(SiO_4)O$ phase and an elevation in its contribution at concentrations above 0.5 M, which causes a rise in the thermophysical parameters and resistance to high-temperature degradation. During the heat resistance tests, it was found that the formation of the composite ceramics with the $Si_3N_4(SiO_2)/Al_2(SiO_4)O/Al_2O_3$ phase composition results in an increase in the stability of their strength properties when exposed to thermally induced oxidation, which has a negative impact on their resistance to softening and a decrease in hardness. Moreover, the presence of the $Al_2(SiO_4)O$ phase in the composition of the ceramics causes a slowdown in the processes of thermal oxidation of the Si_3N_4 phase under prolonged temperature exposure, alongside an increase in the degradation resistance of strength properties by more than 4–7 times, in comparison with the softening data established for single-component ceramics.

Keywords: oxy–nitride ceramics; thermal tests; phase transformations; strength parameters; thermal conductivity; high-strength ceramic materials

Citation: Borgekov, D.B.; Azambayev, S.B.; Kozlovskiy, A.L.; Shlimas, D.I. Effect of Phase Composition Variation of Oxy–Nitride Composite Ceramics on Heat Resistance and Preservation of Strength Parameters. *Crystals* **2024**, *14*, 744. https://doi.org/10.3390/cryst14080744

Received: 4 July 2024
Revised: 15 August 2024
Accepted: 16 August 2024
Published: 21 August 2024

1. Introduction

As is known, today a large share in the field of structural materials is occupied by metal alloys and steels, used in various industries, including in the field of nuclear and alternative energy [1]. However, in view of the latest global trends in the energy sector, associated with the transition to the creation of power plants operating at high temperatures (approximately 1000–1500 °C, and in some cases approximately 2000 °C), the use of traditional metal alloys is impossible due to their low resistance to high-temperature influences [2,3]. The most promising solutions in this direction are composite ceramics that are based on oxide and nitride compounds of aluminum, silicon, zirconium, vanadium, tungsten, and other refractory elements [4–6]. The use of such samples makes it possible to increase the reliability of the operation of structural materials operating at ultra-high

temperatures, as well as to avoid emergency situations associated with the processes of thermal expansion and oxidation. Also, ceramic materials have recently played an important role in the field of creating alternative types of nuclear fuel, due to the need to change the concept of creating a new generation of nuclear reactors, which is based on the need to increase the temperature of the core, as well as the degree of burnup of nuclear fuel, which excludes the possibility of using traditional metal alloys due to their low thermal stability and corrosion resistance [7,8]. In turn, composite ceramics based on oxide and nitride compounds have high inertness to degradation processes, associated with both exposure to aggressive environments and temperature influences, and high strength indicators (hardness, wear resistance, and resistance to cracking and fracture) which allow these ceramics to be used under high mechanical and temperature loads [9,10]. Moreover, in contrast to single-component ceramics with sufficiently low strength indicators, the proposed solution related to the creation of composite ceramics, the manufacturing principle of which is based on the combination of phase transformations and morphological features in order to improve their properties, is one of the most promising solutions in the field of creating structural materials.

Interest in composite ceramics based on compounds of aluminum oxide and silicon nitride is manifested not only when considering these materials as structural materials with higher thermal conductivity and mechanical strength, but also the possibility of creating filter elements based on them, with the possibility of changing their morphological features when varying the ratio of components [11]. The technological process of the synthesis of Al_2O_3–Si_3N_4 ceramics, as a rule, is carried out in a nitrogen atmosphere at elevated temperatures, the main purpose of which is to eliminate the oxidation processes, such as $Si_3N_4 \rightarrow Si_3N_4(SiO_2)$, as well as to preserve the thermophysical properties of silicon nitride. The oxidation process of $Si_3N_4 \rightarrow SiO_2$ itself is caused by the thermodynamic instability of silicon nitride, which is accompanied by oxidation processes, and, therefore, changes in its thermophysical, corrosion, and strength parameters [12].

In one of the first works [13] devoted to the synthesis of Al_2O_3–Si_3N_4 ceramics, it was shown that the use of a stabilizing additive of magnesium oxide at temperatures above 1200 K leads to the formation of glass phases, which subsequently form aluminum-magnesium spinels, as well as the $MgSiO_3$ phase, which has an adverse effect on the strength properties of ceramics. At the same time, annealing in a nitrogen atmosphere made it possible to preserve the a-, β-Si_3N_4 phases in the composition of the ceramics. It should also be noted that, in most cases, the synthesis of composite ceramics based on Al_2O_3–Si_3N_4 compounds is limited to the substitution range within 0.1–0.3 M, the result of which is the production of ceramics with a substitution-type structure or with the formation of (SiAl)(ON) solid solution phases, which have fairly good strength and thermal conductivity, although the oxygen vacancies and defective inclusions associated with the manufacturing processes of ceramics play a major role in determining the thermophysical properties of composite ceramics. [14–16].

The key aim of this study is to determine the influence of phase composition and dimensional factors on the strength and thermophysical properties of composite ceramics based on xAl_2O_3–$(1-x)Si_3N_4$ compounds, as well as maintaining the stability and resistance of the strength and thermophysical parameters to high-temperature influences, accompanied by oxidation processes in the case of prolonged thermal exposure.

The difference of this study is the thermal sintering of xAl_2O_3–$(1-x)Si_3N_4$ ceramics by varying the ratio of components in an oxygen-containing environment, eliminating the need for procedures associated with the nitriding or thermal annealing of ceramics in a nitrogen atmosphere, which makes it possible to reduce the cost of ceramic manufacturing technology, as well as to obtain composite ceramics that combine the properties of silicon nitride and aluminum oxide, alongside the transitional phases associated with the phase transformation processes. Interest in composite ceramics based on oxide and nitride compounds is due to the possibility of using them as solid oxide fuel cells [17], as materials

for energy applications (in particular, as structural materials for new generation nuclear fuel [18–22]), and also as catalysts [23–27].

2. Materials and Methods

The synthesis of the xAl_2O_3–$(1-x)Si_3N_4$ ceramics was carried out using the method of solid-phase mechanochemical grinding, using variations in the stoichiometric ratio of components, the change of which causes phase transformations, as well as variations in strength, optical, and thermophysical parameters. Annealing was carried out in a muffle furnace without pumping out air, i.e., the samples were placed in the furnace chamber, after which the samples were heated at a rate of 20 °C/min and were kept in an air atmosphere. Upon reaching the specified temperature of 1500 °C, the samples were kept for five hours at this temperature, after which the heating was turned off, and the samples remained in the oven for 24 h until completely cooled [24].

The determination of microstructural characteristics was carried out using scanning electron microscopy, implemented using a Phenom™ ProX microscope (Thermo Fisher Scientific, Eindhoven, The Netherlands).

The study of variations in the ratio of components to changes in the phase composition of the xAl_2O_3–$(1-x)Si_3N_4$ ceramics was carried out using the method of X-ray phase analysis.

The structural features associated with the processes of phase transformations in the xAl_2O_3–$(1-x)Si_3N_4$ ceramics, the change of which is caused by deformation processes caused by phase processes of phase formation, were determined through a comparative analysis of the position of the main spectral lines of the Raman spectra, depending on the variation in the concentration of components in the composition of the ceramics.

The thermal conductivity coefficient was measured using a standard method for determining longitudinal heat flow in a wide temperature range, the main purpose of which is to establish the relationship between the influence of phase composition on the mechanisms of heat transfer in ceramics. For measurements, a thermal conductivity meter, KIT-800 (KB Teplofon, Novomoskovsk, Russia), was used.

The determination of the resistance of the ceramics to high-temperature influences leading to the initiation of oxidation processes and the associated degradation of the strength and thermophysical parameters was carried out using a method for simulating the extreme conditions of temperature exposure on the samples under study. Thermal annealing of the samples at temperatures of 700 and 1000 °C was carried out in a Nabertherm LE 4/11/R6 muffle furnace (Nabertherm, Lilienthal, Germany) for 1000 h. Measurements of hardness and cracking resistance were carried out after every 100 h of measurements, which made it possible to evaluate the degradation kinetics of the strength and thermophysical parameters of the ceramics as a result of long-term temperature effects.

Appendix A provides additional information regarding the research methodology and analysis methods.

3. Results and Discussion

The results of the influence of variations in the concentration of the components of the xAl_2O_3–$(1-x)Si_3N_4$ ceramics on the change in grain size (median size) are presented in the form of diagrams of the grain size distribution in Figure 1. Furthermore, the results regarding the dependence of the change in median size on the concentration of the components are presented in Figure 1.

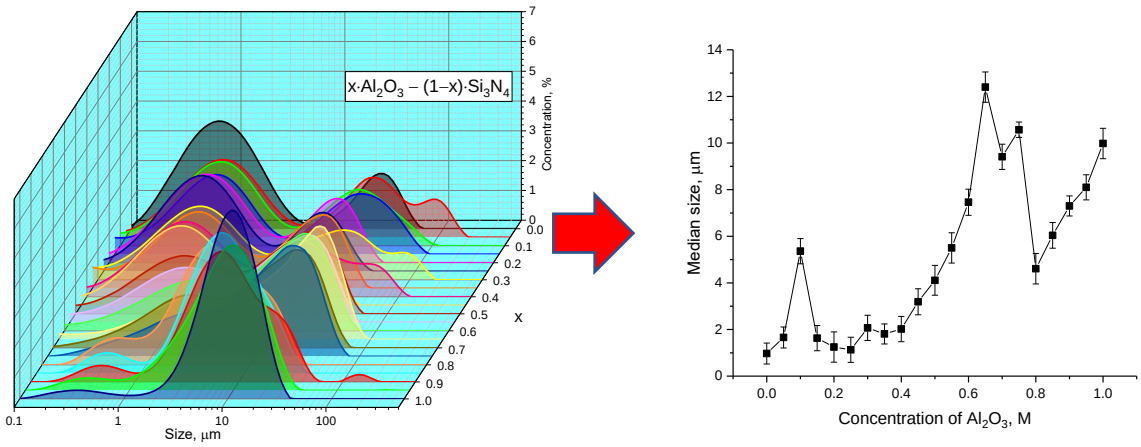

(**a**) (**b**)

Figure 1. (**a**) Distribution of the grains of the studied xAl_2O_3–$(1-x)Si_3N_4$ ceramics, depending on the variation in the ratio of the components; (**b**) dependence of changes in the median grain size in the $(1-x)Si_3N_4$–xAl_2O_3 ceramics, depending on the variation in the ratio of components.

Figure 2 reveals the results of a microstructural analysis of the studied xAl_2O_3–$(1-x)Si_3N_4$ ceramics, contingent upon the variation in the ratio of components, performed using the scanning electron microscopy method. These images reflect changes in the morphology of the resulting ceramics when the ratio of components changes, on the basis of which we can conclude that when the ratio of components varies, there is a change in both the size of the grains and the density of their agglomeration, which consists in the formation of agglomerates of grains united with each other. It is important to highlight that an elevation in the contribution of the Al_2O_3 phase results in enlargement of the grains, the shape of which is characteristic of the Al_2O_3 phase (in comparison with the initial data for samples of single-component Al_2O_3 ceramics).

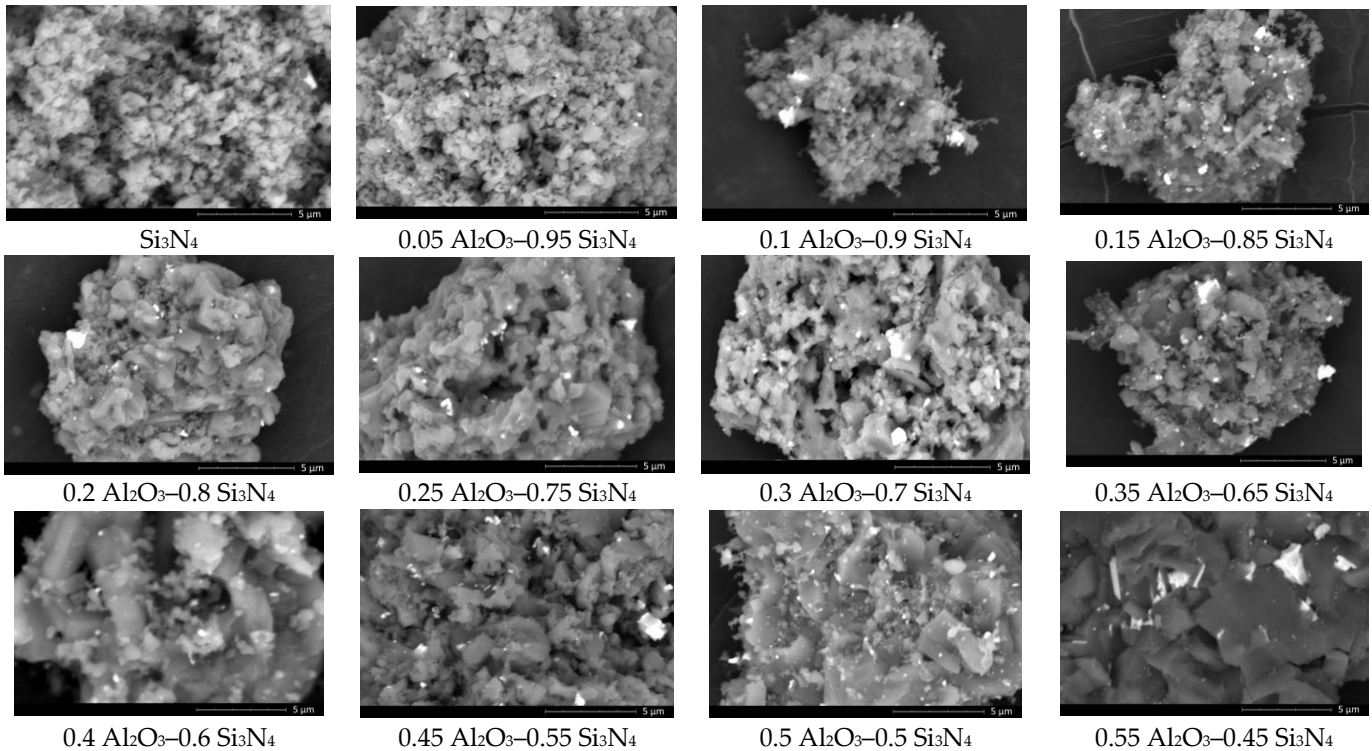

Figure 2. *Cont.*

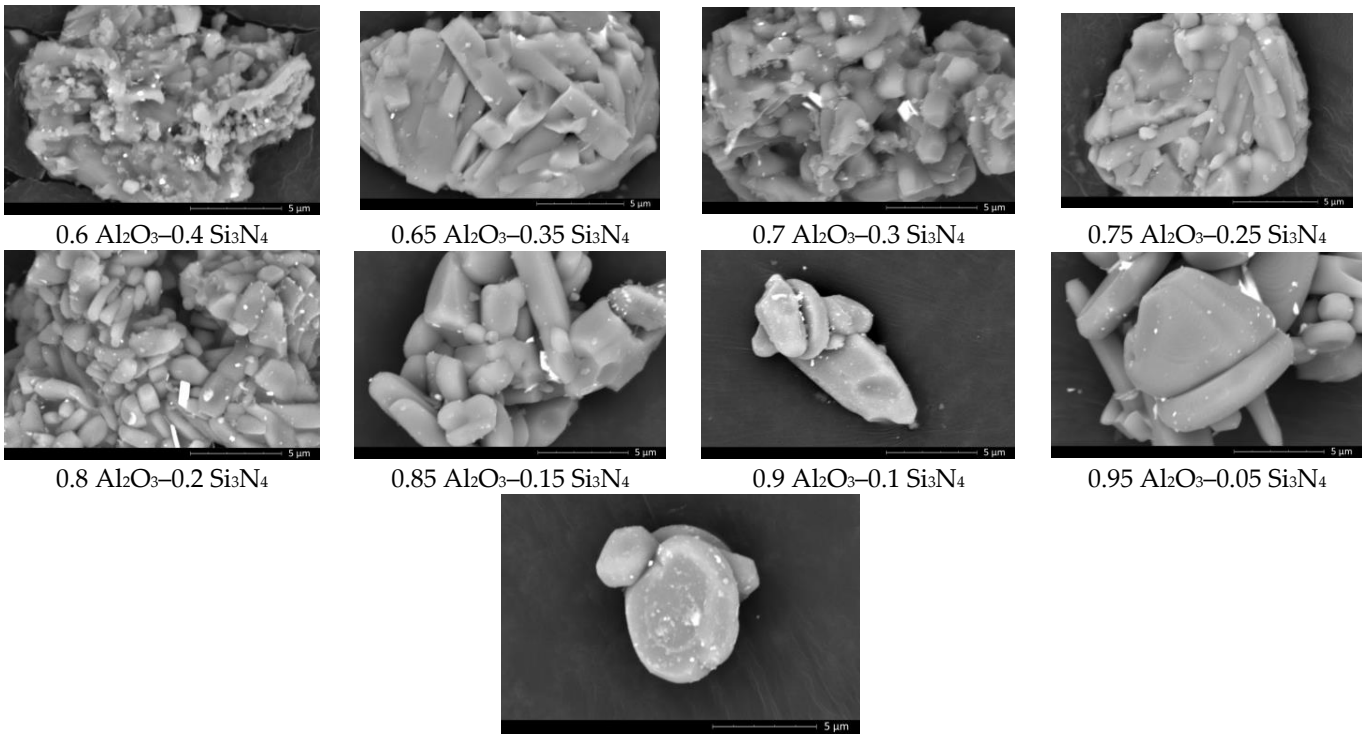

Figure 2. Results of a microstructural analysis of the studied $xAl_2O_3–(1−x)Si_3N_4$ ceramics.

Figure 3 reveals the results of an X-ray phase analysis of the studied $xAl_2O_3–(1−x)Si_3N_4$ ceramics depending on the variation of the components. Descriptions of the results of the morphological features that are associated with changes in the median grain size (see the data in Figure 1a) as well as of the phase transformations caused by changes in the ratio of components are given together to determine the relationship between morphological features and the phase composition of the ceramics. The presence of two or more phases in the composition of the ceramics, depending on the variation of the components having different grain sizes, as well as the dynamics of changes in their contributions, is clearly visible in the presented grain distribution diagrams. According to the diagrams, variation in the concentration of the components in the composition of the ceramics leads to the displacement of fine grains, the sizes of which are in the order of 0.3–2 microns, followed by their subsequent agglomeration into larger grains with sizes in the order of 5–15 microns.

The observed oxidation processes associated with the formation of the SiO_2 phase, in the case of silicon nitride without the addition of aluminum oxide, is due to the effect of the partial decomposition and subsequent replacement of nitrogen with oxygen in the structure of silicon nitride, which leads to the formation of inclusions in the form of SiO_2. This effect is due to the conditions of thermal annealing in an oxygen-containing environment, which leads to the possibility of introducing oxygen into silicon nitride, with the subsequent formation of an impurity phase SiO_2. When 0.05 M Al_2O_3 is added to silicon nitride, the resulting X-ray diffraction patterns do not reveal the presence of reflections that are characteristic of aluminum oxide phases, and the main alterations are associated with changes in the weight contributions of the previously established tetragonal SiO_2 and hexagonal Si_3N_4 phases, which indicates that the phase transformation processes are associated with the formation of the oxide phase SiO_2. At the same time, the analysis of changes in the median grain size (see data in Figure 1b) indicates a slight increase in size, which can be explained by the effects of agglomeration during the formation of the SiO_2 phase.

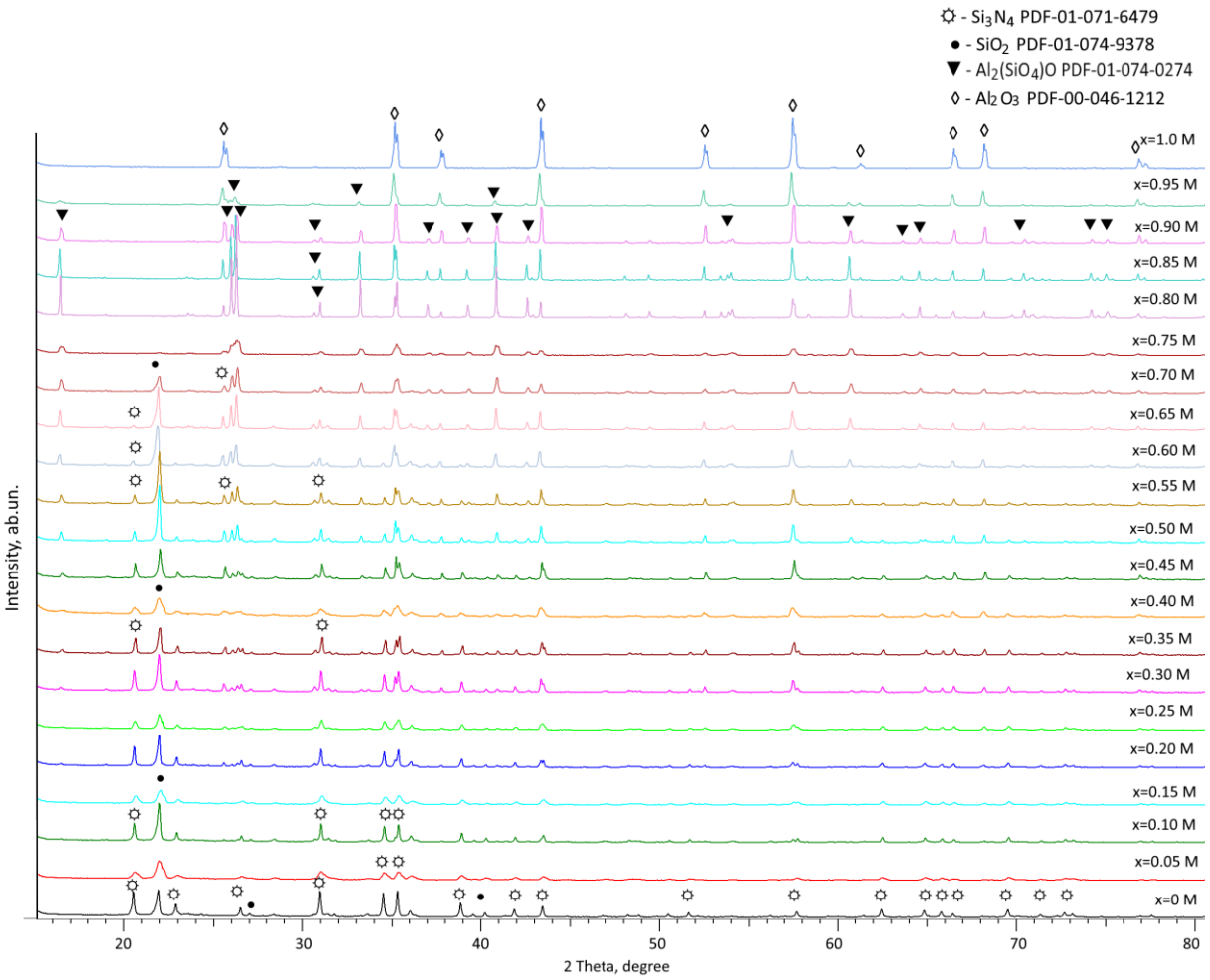

Figure 3. Results of the X-ray diffraction of the studied xAl_2O_3–$(1-x)Si_3N_4$ ceramics in the case of variation of the ratio of the components in the composition.

The presence of a local maximum in the presented graph of the median grain size in the ceramics at an Al_2O_3 concentration of 0.1 M may be due to the effect associated with the formation of the hexagonal solid solution phase (SiAl)(ON), the formation of which is observed only at this Al_2O_3 concentration, and with a further increase in concentration, the formation of a stable Al_2O_3 phase with an orthorhombic crystal lattice is observed (according to the X-ray phase analysis data). The very formation of this phase of the solid solution (SiAl)(ON) is due to the partial replacement of the Si–N bonds with Al–O bonds in Si_3N_4 [28]. It should be noted that the presence of this phase, observed only at low concentrations of Al_2O_3, can be explained by the fact that at a low concentration of aluminum oxide, the formation of a stable Al_2O_3 phase in the composition does not occur, and the phase formation process is accompanied not only by transformations of the $Si_3N_4 \xrightarrow{1500\,^{\circ}C} Si_3N_4/SiO_2$ type, but also by the partial replacement of bonds, with the subsequent displacement of inclusions from Si_3N_4 in the form of (SiAl)(ON) grains. In turn, anomalous grain growth may be due to the effects of agglomeration and adhesion due to the presence of a transitional phase (SiAl)(ON). The presence of this phase in the synthesis of Al_2O_3–Si_3N_4 ceramics, in the case of adding a low concentration of nanosized Al_2O_3 particles, was shown in [29]. At the same time, the authors also identified reflections that were characteristic of the Si_2N_2O phase, the formation of which is associated with thermal exposure at a temperature of 1650 °C in a nitrogen atmosphere.

At an Al_2O_3 concentration of 0.3 M, thermal annealing leads to the formation of the orthorhombic phase $Al_2(SiO_4)O$, which adheres to the spatial system of Pbnm(62)

(PDF-01-074-0274), the formation of which occurs as a result of the interaction of silicon oxide formed as a result of the phase transformation of $Si_3N_4 \xrightarrow{1500\,^{\circ}C} Si_3N_4/SiO_2$ with the aluminum oxide phase (PDF-00-046-1212), stable reflections of which are recorded at an Al_2O_3 concentration of 0.2 M and higher. It should be noted that a change in the ratio of the components associated with a rise in the contribution of Al_2O_3 leads to the preservation of the trend of phase transformations of silicon nitride of the $Si_3N_4 \xrightarrow{1500\,^{\circ}C} Si_3N_4/SiO_2$ type, and the trend in the content of the silicon oxide phase in the composition decreases slightly, due to the fact that most of this oxide is involved in the formation of the $Al_2(SiO_4)O$ phase. At Al_2O_3 concentrations above 0.7 M, the contribution of the Si_3N_4 phase in the composition of the ceramics, according to the X-ray phase analysis data, is not observed, nor is the contribution of the SiO_2 phase, which indicates that at low concentrations of Si_3N_4 (no more than 0.3 M), thermal annealing leads to a complete transformation of $Si_3N_4 \rightarrow SiO_2$, which in turn participates in the formation of the $Al_2(SiO_4)O$ phase. At the same time, a growth in Al_2O_3 concentration above 0.8 M results in coarsening of the grain sizes (see data presented in Figure 1a,b), which implies the enlargement of agglomerates due to the displacement of the $Al_2(SiO_4)O$ phase and the dominance of the Al_2O_3 phase in the composition of the ceramics.

Based on a comprehensive analysis of the obtained series of X-ray diffraction patterns, changes in the phase composition were determined in the case of varying the ratio of the components in the composition of the xAl_2O_3–$(1-x)Si_3N_4$ ceramics, the results of which are presented in Figure 4. The determination of the weight contributions of each phase was carried out by determining the contribution of the areas of diffraction reflections for each established phase on the X-ray diffraction pattern, followed by recalculation of the contributions, considering the corundum numbers taken from the PDF-2 database. According to the presented diagram, it is possible to determine the main phase changes associated with the processes of phase formation with a variation in the ratio of the components in the composition of the ceramics, as well as to establish the phase transformation dynamics in the ceramics, the general form of which can be presented as follows (1):

$$\begin{aligned} Si_3N_4(SiO_2) &\xrightarrow{0.05-0.15\ M\ Al_2O_3} Si_3N_4(SiO_2)/(SiAl)(ON) \xrightarrow{0.20-0.75\ M\ Al_2O_3} \\ Si_3N_4(SiO_2)/Al_2(SiO_4)O/Al_2O_3 &\xrightarrow{0.8-0.95\ M\ Al_2O_3} Al_2(SiO_4)O/Al_2O_3. \end{aligned} \quad (1)$$

Table A1 in Appendix B shows the crystal lattice parameters for all of the established phases depending on the concentration of the components in the ceramic composition, reflecting changes in the structural parameters associated with phase formation processes. Figure 5a,b illustrates the assessment results of the changes in material density and porosity, calculated based on data comparing the density of samples obtained by measurements using the Archimedes method and theoretical values of the density of samples. As is evident from the presented dependences of the change in density, the formation of the $Al_2(SiO_4)O$ and Al_2O_3 phases with a change in Al_2O_3 concentrations leads to only small changes in the density of the ceramics from 3.3 to 3.45 g/cm^3, which are caused by a change in the ratio of the phases in the composition. In this case, an increase in the contribution of the Al_2O_3 phase results in an increase in the ceramic density, which is due to a higher density of Al_2O_3 (ρ_{Al2O3} = 3.98 g/cm^3). Figure 5b shows the results of a comparative analysis of the change in the density of the studied samples, obtained using the Archimedes method with the calculated data obtained on the basis of the structural analysis data. As can be seen from the presented data, changes in the phase composition lead to a decrease in the difference in density values, which allows us to judge the convergence of the density results that were obtained using the Archimedes method and the structural analysis data.

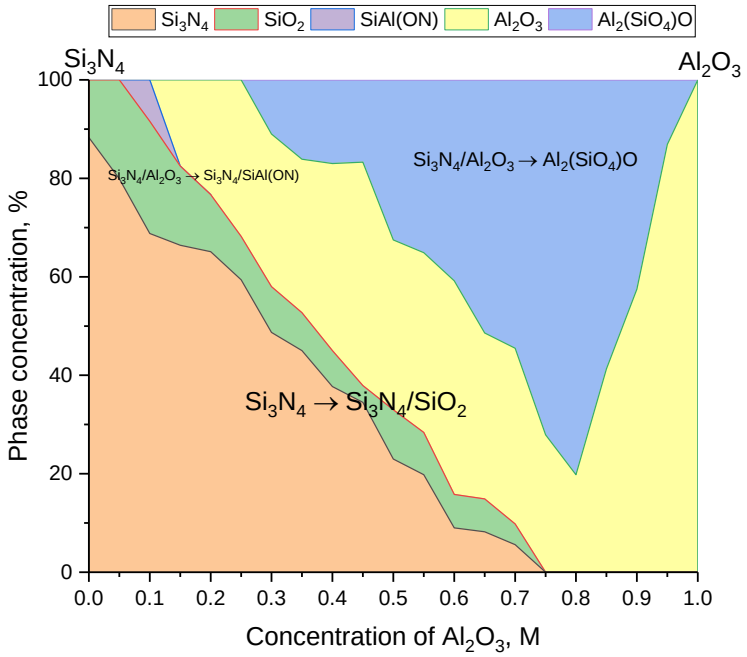

Figure 4. Phase diagram of the xAl_2O_3–$(1-x)Si_3N_4$ ceramics in the case of variation in the concentration of the components during thermal annealing.

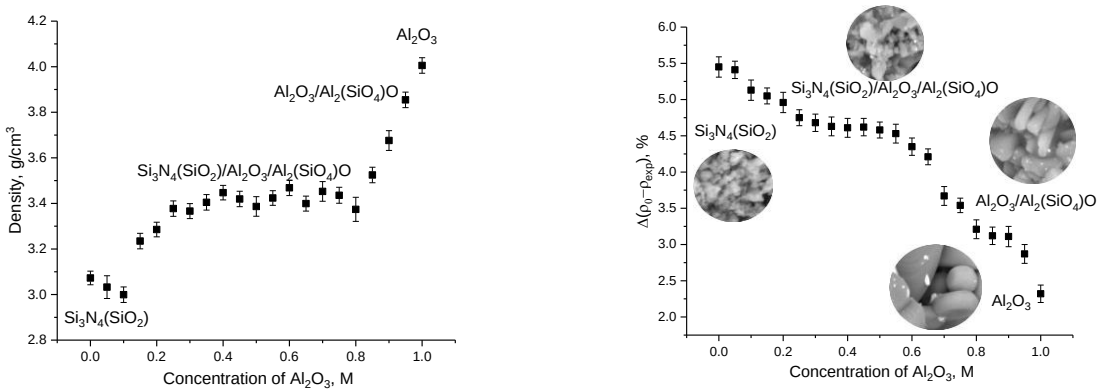

(**a**) (**b**)

Figure 5. (**a**) Results of a density analysis of the studied xAl_2O_3–$(1-x)Si_3N_4$ ceramics; (**b**) $\Delta(\rho_0 - \rho_{exp})$ assessment results for the xAl_2O_3–$(1-x)Si_3N_4$ ceramics.

Figure 6 demonstrates the results of Raman spectroscopy of the studied xAl_2O_3–$(1-x)Si_3N_4$ ceramics depending on the variation in the concentration of the components, which reflect the change in the fundamental modes associated with the formation of phases and their structural ordering. The spectra of Si_3N_4 without the addition of Al_2O_3 contain peaks at 253, 357, and 497 cm^{-1}, which may belong to the α-Si_3N_4 phase. Peaks at 253 and 497 cm^{-1} correspond to the A_{1g} modes, and a peak at 357 cm^{-1} corresponds to the E_g mode [30]. In addition, low-intensity peaks at 178, 196, and 224 cm^{-1} can be associated with the β-Si_3N_4 phase [31]. The peak in the region of 800 cm^{-1} is characteristic of the SiO_2 phase, the formation of which occurs as a result of the oxidation process under the thermal influence associated with the processes of replacing nitrogen with oxygen, with the subsequent formation of inclusions in the form of SiO_2 [32]. At Al_2O_3 concentrations in the x range from 0.05 M to 0.50 M, the spectra change only slightly; small fluctuations in peak intensity are observed only in the region of 650–950 cm^{-1}. When the Al_2O_3 concentration reaches x = 0.55, peaks appear at 800 and 880 cm^{-1}, which can be associated with the

$Al_{4+2x}Si_{2-2x}O_{10-x}$ phase, the weight contribution of which increased, according to X-ray phase analysis. At a concentration of x = 0.70 M, fluorescence begins to appear in the region of 1200–1800 cm^{-1}, which may be due to the high corundum content in the samples. At Al_2O_3 concentration x = 0.90 M, a peak appears at 412 cm^{-1} corresponding to the A_{1g} mode of the α-Al_2O_3 phase [33].

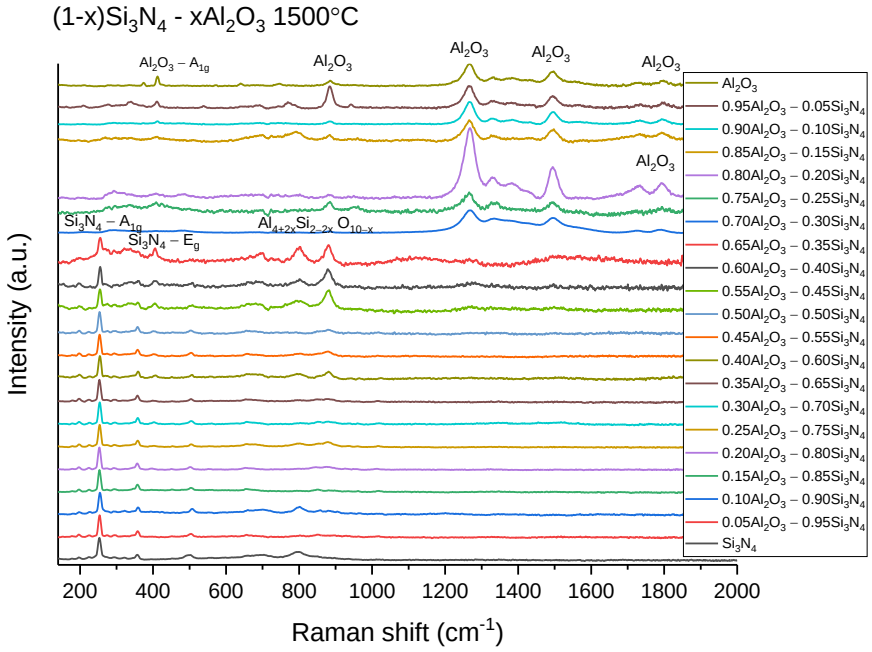

Figure 6. Raman spectra of the xAl_2O_3–$(1-x)Si_3N_4$ ceramics, depending on the concentration of the components in the composition of the ceramics.

Thus, analyzing the data from the X-ray phase analysis and Raman spectroscopy, it can be concluded that the observed changes are in good agreement with each other, and that both methods together make it possible to determine with sufficiently high accuracy the dynamics of phase transformations in the ceramic samples, depending on the variation in the ratio of the components in the composition.

Figure 7 illustrates the results of hardness measurements of the studied xAl_2O_3–$(1-x)Si_3N_4$ ceramics in the case of a change in the ratio of components, and as a consequence, variations in the phase composition of the ceramics. The general view of the presented dependence of the change in hardness of the xAl_2O_3–$(1-x)Si_3N_4$ ceramics with variation in the ratio of the components has a clear dependence on both the phase transformations that occur in the ceramics and the phase content, the change in which causes the hardening effect in comparison with the hardness data for Si_3N_4. The observed changes in hardness at Al_2O_3 concentrations equal to 0.05–0.1 M are due to small changes in the Si_3N_4/SiO_2 phase ratio, the alteration of which occurs as a result of the thermal decomposition processes of $Si_3N_4 \overset{1500\,^{\circ}C}{\rightarrow} Si_3N_4/SiO_2$. At the same time, the most significant changes in hardness are observed during the formation of the $Al_2(SiO_4)O$ phase in the ceramics, an increase in the contribution of which leads to the strengthening of the ceramics by more than 1.4 times compared to the hardness data for the Si_3N_4 samples. At the same time, the obtained hardness values for the xAl_2O_3–$(1-x)Si_3N_4$ ceramics at Al_2O_3 concentrations above 0.4 M are in good agreement with the literature data from [28–30], in which hardening is caused by both the dimensional factors that are associated with the presence of fine or nanosized grains and with the phase transformations that are caused by changes in the phase ratio in the composition of the ceramics. Displacement of the $Al_2(SiO_4)O$ phase at low concentrations of Si_3N_4 in the ceramic composition leads to a decrease in hardness, which is due to lower hardness values for the Al_2O_3 phase, which is dominant in the ceramic composition.

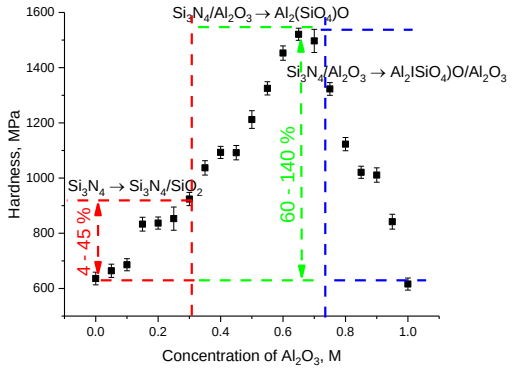

Figure 7. Results of changes in the hardness of the xAl_2O_3–$(1-x)Si_3N_4$ ceramics, depending on the concentration of the components in the composition.

Figure 8a reveals the results of the measurements of the thermal conductivity of the xAl_2O_3–$(1-x)Si_3N_4$ ceramics under study, depending on the variation in the ratio of the components in the composition. To compare the results of the changes in the thermal conductivity coefficient, we selected works in which the thermophysical parameters of similar ceramics that were obtained using the methods of mechanical mixing and thermal annealing were studied [31–37].

As is known, polycrystalline Si_3N_4 ceramics obtained by hot pressing under high pressure, which eliminates the processes of oxidation and the formation of oxide inclusions in the composition, as well as oxygen vacancies, have fairly good thermal conductivity, which in turn leads to a pronounced dependence on the concentration of defects and oxygen vacancies in the composition [34]. In this case, thermal annealing of mechanically deformed Si_3N_4 powders, accompanied by the decomposition of the $Si_3N_4 \rightarrow SiO_2$ type, leads to the presence of oxygen and silicon vacancies, the formation of which occur according to the mechanism of maintaining electrical neutrality when oxygen replaces nitrogen atoms, with the subsequent formation of vacancies in the silicon sublattice ($2O_2 \rightarrow 4O^{*}_{N} + V_{Si}^{''''}$) [35]. As a result, the value of the thermal conductivity coefficient for the Si_3N_4 ceramics is about 1.76 W/(m × K). At the same time, comparing the results of changes in thermal conductivity for Si_3N_4 ceramics from this work and work [32], it can be concluded that thermal annealing of the samples at a temperature of 1500 °C, in comparison with conventional stirring and pressing, makes it possible to more than triple the thermal conductivity of the ceramics by reducing deformation distortions, which are observed as scattering centers and vacancies. The addition of low Al_2O_3 content ceramics to the Si_3N_4 composition (at concentrations from 0.05 to 0.15 M) does not lead to significant changes in the thermal conductivity coefficient (ΔTC~2–6%), which indicates that the absence of any significant changes in the phase composition associated with the formation of replacement phases does not have a significant effect on changes in the thermophysical parameters. The most significant changes in thermal conductivity occur at Al_2O_3 concentrations above 0.15 M, which are characterized by the formation of the $Al_2(SiO_4)O$ phase, the appearance of which in the composition of ceramics leads to an increase in the thermal conductivity coefficient from 1.76–1.79 W/(m × K) to 2.56–2.78 W/(m × K), which is more than a 1.5-fold increase in thermal conductivity. At the same time, a trend of increasing thermal conductivity, depending on the variation in the concentration of the components in the ceramic composition, is observed up to Al_2O_3 concentrations equal to 0.6–0.65 M, for which, according to the X-ray phase analysis, the presence of inclusions in the form of silicon nitride in the composition is observed. This growth in thermal conductivity can be explained by several factors. Firstly, according to the X-ray phase analysis data, a change in the phase composition through the formation of the $Al_2(SiO_4)O$ phase results in a porosity decrease, associated both with a change in the density of the ceramics and with size effects caused by the packing density of the grains in the ceramic composition. Secondly, the stabilization of structural parameters due to phase formation processes reduces the concentration of defective inclusions in the composition of

the ceramics and also contributes to a change in the number of vacancies, which in turn provides a smaller number of scattering centers that impede heat transfer.

In the case of the concentration of silicon nitride in the composition of xAl_2O_3–$(1-x)Si_3N_4$ ceramics being less than 0.35 M, according to the X-ray phase analysis data, the Al_2O_3 phase begins to dominate in the composition, which in turn leads to an increase in porosity (according to the porosity measurements taken using the Archimedes method), as well as an enlargement of grain sizes. It should be noted that the observed changes in thermal conductivity in the case of low Al_2O_3 concentrations are in good agreement with the results of other works, while the proposed method for producing ceramics, which eliminates a large number of technological operations, makes it possible to obtain ceramics with fairly high thermal conductivity in comparison with other oxide ceramics, such as ZrO_2 (0.3–3.2 W/(m × K) depending on density and porosity [36]) and ZrO_2–Al_2O_3 (approximately 2.5–4.5 W/(m × K) depending on the ratio of components [37]). Moreover, in a number of works [33,38,39], it was shown that the thermal conductivity of ceramics has a direct dependence not only on the concentration of vacancies and defects in the composition but also on porosity. In the case of high porosity, the observed reduction in thermal conductivity is due to a large number of voids, which interferes with the mechanisms of phonon heat transfer and reduces the rate of heat transfer. Direct confirmation of this is the presented comparative analysis of the porosity values and the efficiency of changing the thermal conductivity coefficient, presented in Figure 8b.

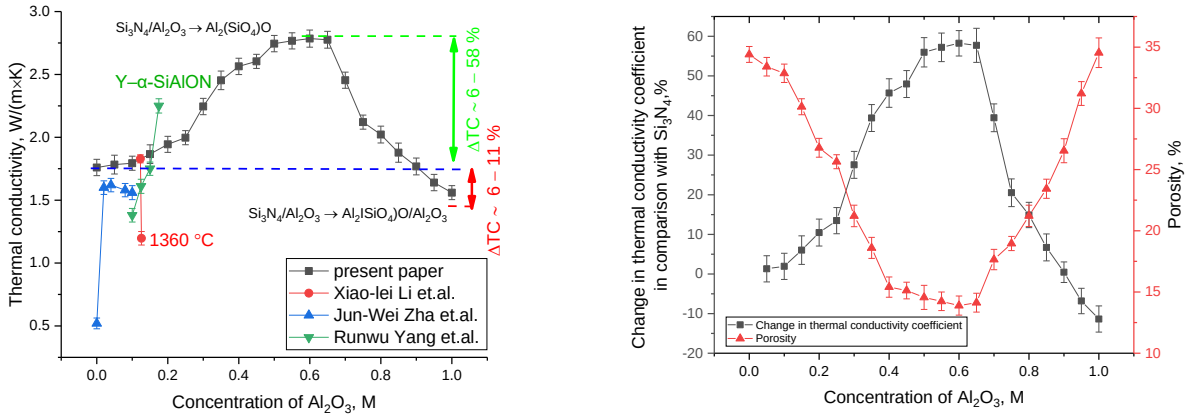

Figure 8. (**a**) Results of the analysis of the thermal conductivity of the xAl_2O_3–$(1-x)Si_3N_4$ ceramics, depending on the concentration of the components in the composition (data are presented in comparison with the results of other works [33,38,39]); (**b**) comparison of the results of changes in the thermal conductivity and porosity of the xAl_2O_3–$(1-x)Si_3N_4$ ceramics, depending on the concentration of the components in the composition.

An important factor determining the prospects for using composite heat-resistant ceramics is the assessment of their resistance to high-temperature influences and thermal shocks, as well as maintaining the stability of the strength properties of the ceramics to such influences. For example, in [40], it was shown that thermal heating leads to a decrease in fracture resistance by more than 400 °C, and the main effect causing such a strong decrease in strength properties is due to the ratio of cations/anions in the composition of the ceramics, the presence of which are associated with the phase composition causing changes in the coefficient of thermal expansion.

Figure 9 illustrates the results of the measurements of the hardness of the ceramic samples, depending on the variation of the components in the composition, obtained during life tests to determine the stability of the strength parameters to long-term thermal effects and the associated oxidation processes. The general trend of the changes in hardness at a test temperature of 700 °C indicates a fairly high resistance of the ceramics to long-

term thermal effects, especially for the ceramics that were obtained with an Al_2O_3 content of 0.3–0.6 M. The least stable ceramics were the single-component ceramics, which in turn confirms the applicability of the concept of creating composite ceramics that have higher resistance to external influences compared to single-component ceramics. At a test temperature of 1000 °C, the decrease in hardness during life tests became more pronounced, which in turn may be due to more intense oxidation processes of silicon nitride at high temperatures. A change in hardness, indicating softening and a decrease in resistance to mechanical external influences, in the case of a test temperature of 1000 °C is observed after 400–500 h of successive thermal exposure, which also confirms the fact that with the increase in exposure temperature, the degradation rate of strength properties increases and becomes more pronounced with prolonged exposure.

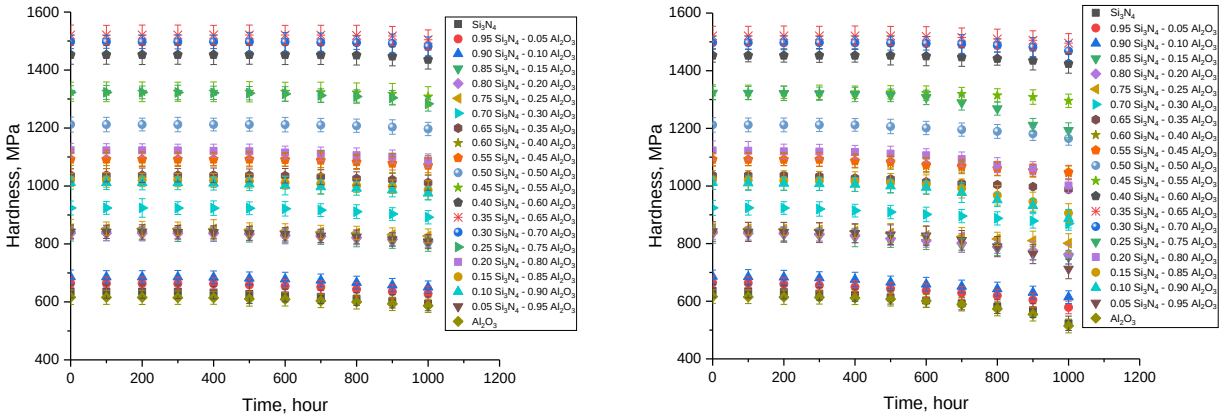

(**a**) (**b**)

Figure 9. Results of changes in the hardness of the xAl_2O_3–$(1-x)Si_3N_4$ ceramics during heat resistance tests at different annealing temperatures: (**a**) at an annealing temperature of 700 °C; (**b**) at an annealing temperature of 1000 °C.

Figure 10 demonstrates the results of a comparative analysis of the degradation of hardness values as a result of thermal tests associated with oxidation processes. The hardness degradation was determined by comparing hardness values before and after heat resistance tests (after 1000 h) with the subsequent calculation of deviations from the initial value considering measurement error.

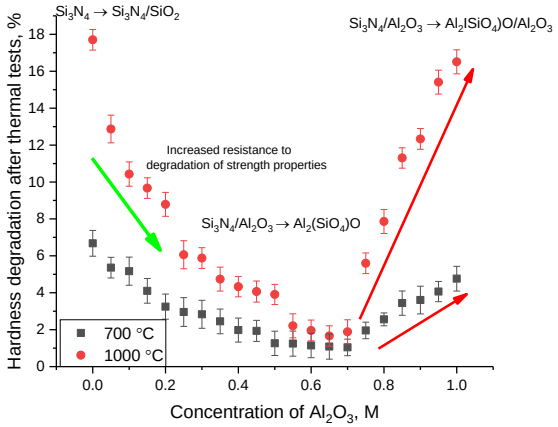

Figure 10. Results of a comparative analysis of changes in hardness after thermal tests, depending on the concentration of the components in the composition of the xAl_2O_3–$(1-x)Si_3N_4$ ceramics.

As can be seen from the data presented, the formation of the $Al_2(SiO_4)O$ phase in the composition of the ceramics with a subsequent increase in its content and a decrease in

the weight contribution of the Si_3N_4 phase due to phase transformations leads to a growth in resistance to softening by more than 4–7 times in comparison with the softening data that was established for the single-component ceramics. Such obvious differences in the change in hardness may be associated with the processes of the high-temperature oxidation of silicon nitride, which lead to softening of the ceramics due to a rise in the SiO_2 phase, as well as its structural disorder.

The degradation kinetics of the ceramics, contingent upon the temperature of life tests, were determined by the assessment of the phase composition of the ceramics before and after thermal exposure for 1000 h at different temperatures. The results are presented in the form of diagrams in Figure 11, reflecting the change in the phase ratio associated with oxidation processes.

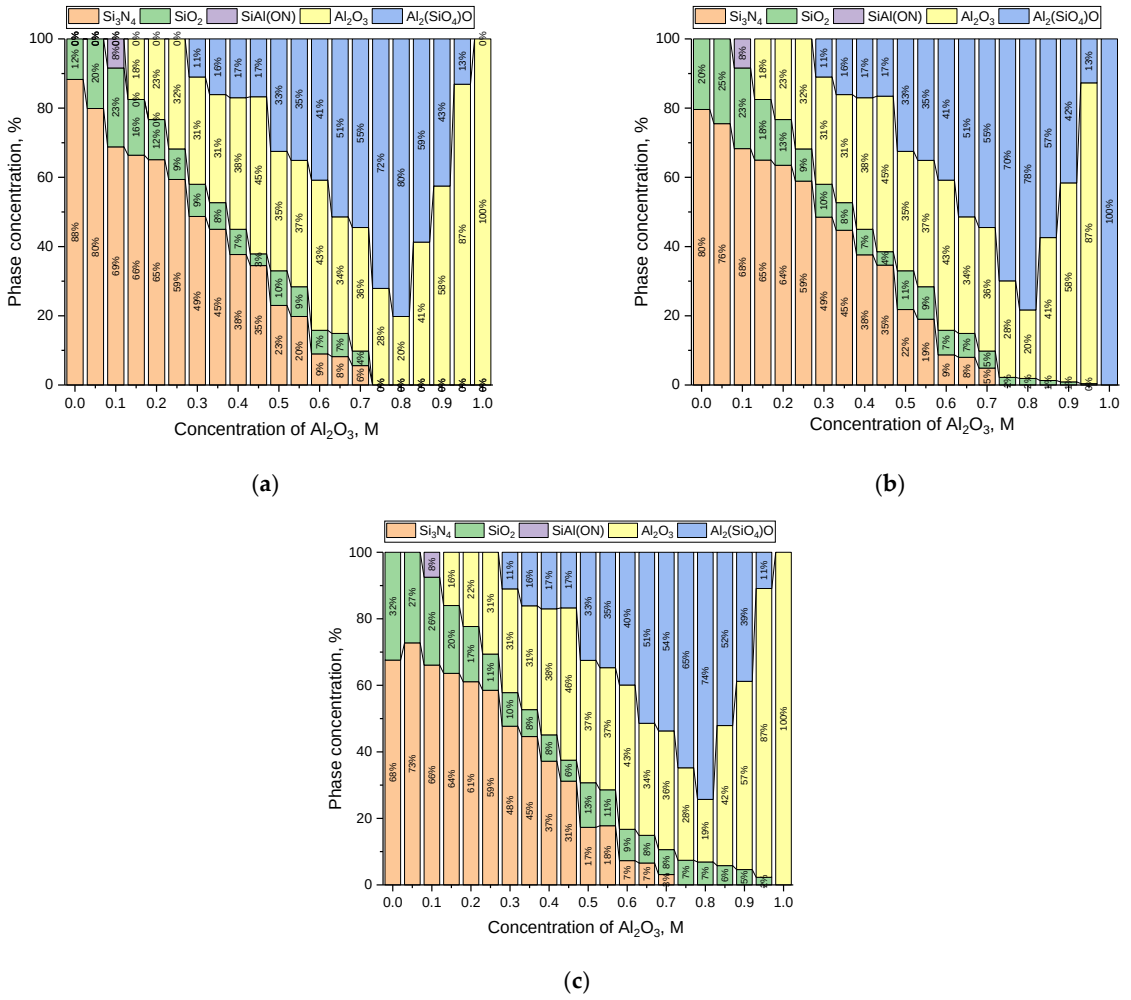

Figure 11. Results of changes in the phase composition of the xAl_2O_3–$(1-x)Si_3N_4$ ceramics before and after thermal tests: (**a**) pristine; (**b**) at an annealing temperature of 700 °C; and (**c**) at an annealing temperature of 1000 °C.

According to the data obtained, the most significant changes in the phase composition are observed for the ceramics that were subjected to thermal action at a temperature of 1000 °C and are associated with an increase in the contribution of the SiO_2 phase. The growth in SiO_2 content that was observed for the high-temperature tests is due to the oxidation processes of the Si_3N_4 phase, which is most pronounced at low contents of the Al_2O_3 phase, and less pronounced (the change is no more than 1.0–1.5%) for samples in which the formation of the $Al_2(SiO_4)O$ phase, which has higher resistance to high-temperature corrosion compared to silicon nitride, which is oxidized under the influence of

temperature by replacing nitrogen with oxygen with the subsequent formation of silicon dioxide, was observed. Thus, by analyzing the phase changes in the ceramics as a result of thermal effects, we can conclude that the presence of two or more phases in the composition of the ceramics leads to an increase in the stability of the ceramics to oxidation, in particular, a slowdown in the oxidation process of silicon nitride, as well as the maintenance of the stability of the $Al_2(SiO_4)O$ phase in the case of low silicon nitride contents in the composition of the initial mixture. At the same time, the limiting factor to oxidation and the subsequent degradation of strength properties (reduction of hardness) is the presence of the $Al_2(SiO_4)O$ phase in the composition of the ceramics, the presence of which also determines higher strength and thermal conductivity. Maintaining the oxidation stability of the composite ceramics at high temperatures, in turn, can be explained by them having higher thermal conductivity, which ensures uniform heat distribution and transfer during prolonged temperature exposure.

4. Conclusions

This paper presents the results of a comprehensive analysis of the phase transformations, strength properties, and heat resistance of composite xAl_2O_3–$(1-x)Si_3N_4$ ceramics. Using the method of X-ray phase analysis and Raman spectroscopy, the results of the influence of variations in the ratio of the components in the composition of the xAl_2O_3–$(1-x)Si_3N_4$ ceramics on changes in the phase composition obtained using the method of mechanochemical solid-phase synthesis were obtained. During the determination of the thermophysical parameters, it was found that the formation of the $Al_2(SiO_4)O$ phase in the ceramics, an elevation in the contribution of which results in porosity reduction, causes a rise in the thermal conductivity coefficient by 10–60% in comparison with the thermal conductivity of single-component Si_3N_4 and Al_2O_3 ceramics, the low values for which are due to high porosity. During the tests, it was established that the presence of the $Al_2(SiO_4)O$ phase in the composition of the xAl_2O_3–$(1-x)Si_3N_4$ ceramics in combination with the Si_3N_4 phase leads to a rise in the resistance to high-temperature oxidation, resulting in softening of the ceramics. Moreover, the presence of the $Al_2(SiO_4)O$ phase in the composition of the ceramics causes an increase in strength and thermophysical properties, which allows for expanding the potential for using these ceramics as structural materials.

Author Contributions: Conceptualization, D.B.B., S.B.A., D.I.S. and A.L.K.; methodology, D.B.B., S.B.A., D.I.S. and A.L.K.; formal analysis, D.I.S. and A.L.K.; investigation, D.B.B., S.B.A. and D.I.S.; resources, D.B.B. and A.L.K.; writing—original draft preparation, review, and editing, D.B.B., S.B.A., D.I.S. and A.L.K.; visualization, S.B.A. and A.L.K.; supervision, D.B.B. All authors have read and agreed to the published version of the manuscript.

Funding: This study was funded by the Ministry of Education and Science of the Republic of Kazakhstan (grant AP14871176).

Data Availability Statement: Dataset available on request from the authors.

Conflicts of Interest: The authors declare no conflicts of interest.

Appendix A

Mechanochemical grinding of the studied ceramics was carried out in a planetary mill PULVERISETTE 6 (Fritsch, Berlin, Germany) using the following mode: 250 rpm, grinding for 30 min. For grinding, a glass (cylindrical container made of tungsten carbide with a diameter of 10 cm and a height of 7 cm) and grinding balls (the diameter of the balls was 10 mm) made of tungsten carbide were used, which have high mechanical strength to abrasion, which eliminates the effect of impurities getting into the grinding composition. The choice of grinding mode was based on the need to create a powder that is homogeneous in composition, as well as to initialize the mechanically induced deformation distortion of the crystal structure of the powders being ground, the relaxation of which under high temperature exposure contributes to the initialization of the phase transformation pro-

cesses. The initialization of the phase transformation processes, depending on variations in the concentration of the components in the ceramic composition, was carried out in a Nabertherm LE 4/11/R6 muffle furnace (Nabertherm, Lilienthal, Germany).

The determination of the weight contributions of each established phase was carried out by clarifying the areas of all diffraction reflections that are characteristic of a given phase, followed by calculating their contribution in the overall diffraction pattern, considering the corundum numbers for each phase, alongside background radiation. The phase refinement was made considering a priori information about the phase transformation processes in ceramics under thermal influence when changing the ratio of components, as well as a full-profile analysis of the obtained diffraction patterns. Data for the full profile analysis were taken from the PDF-2 (2016) database.

An Enspectr M532 (Spectr-M LLC, Chernogolovka, Russia) was used to measure the Raman spectra. The spectra were obtained using a laser with a wavelength of λ = 785 nm.

The measurements were carried out on samples in the form of tablets with a diameter of 10 mm and a thickness of about 1 mm. These tablets were pressed under a pressure of 200 MPa for 30 min, after which they were annealed for 5 h at a temperature of 400 °C in order to remove mechanically initiated deformation structural distortions.

Appendix B

Table A1. Data on the structural parameters of the studied ceramics, depending on the ratio of the components.

Concentration of Al_2O_3, M	Lattice Parameter, Å				
	Si_3N_4	SiO_2	(SiAl)(ON)	$Al_2(SiO_4)O$	Al_2O_3
0	a = 7.7632 ±0.0015 Å, c = 5.6247 ± 0.0014 Å	a = 4.9796 ± 0.0014 Å, c = 6.9512 ± **0.0016 Å**	-	-	-
0.05	a = 7.7417 ± 0.0011 Å, c = 5.5937 ± 0.0018 Å	a = 4.9611 ± 0.0014 Å, c = 6.9481 ± 0.0012 Å	-	-	-
0.10	a = 7.7433 ± 0.0016 Å, c = 5.6157 ± 0.0014 Å	a = 4.9689 ± 0.0016 Å, c = 6.9263 ± 0.0013 Å	a = 7.5981 ± 0.0014 Å, c = 2.9060 ± 0.0013 Å	-	-
0.15	a = 7.7204 ± 0.0018 Å, c = 5.5761 ± 0.0013 Å	a = 4.9416 ± 0.0012 Å, c = 6.9344 ± 0.0017 Å	-	-	a = 4.7354 ± 0.0017 Å, c = 12.9598 ± 0.0014 Å
0.20	a = 7.7493 ± 0.0016 Å, c = 5.5981 ± 0.0014 Å	a = 4.9729 ± 0.0014 Å, c = 6.9426 ± 0.0021 Å	-	-	a = 4.7468 ± 0.0017 Å, c = 13.0005 ± 0.0022 Å
0.25	a = 7.7478 ± 0.0025 Å, c = 5.6136 ± 0.0021 Å	a = 4.9669 ± 0.0013 Å, c = 6.9344 ± 0.0022 Å	-	-	a = 4.7466 ± 0.0016 Å, c = 12.9751 ± 0.0013 Å
0.30	a = 7.7463 ± 0.0016 Å, c = 5.6155 ± 0.0012 Å	a = 4.9756 ± 0.0017 Å, c = 6.9425 ± 0.0021 Å	-	a = 7.5311 ± 0.0016 Å, b = 7.6813 ± 0.0014 Å, c = 5.7461 ± 0.0014 Å	a = 4.7531 ± 0.0017 Å, c = 12.9825 ± 0.0026 Å
0.35	a = 7.7281 ± 0.0015 Å, c = 5.6003 ± 0.0014 Å	a = 4.9553 ± 0.0016 Å, c = 6.9317 ± 0.0013 Å	-	a = 7.5164 ± 0.0017 Å, b = 7.5164 ± 0.0022 Å, c = 6.7551 ± 0.0014 Å	a = 4.7382 ± 0.0015 Å, c = 12.9904 ± 0.0013 Å
0.40	a = 7.7645 ± 0.0017 Å, c = 5.5959 ± 0.0021 Å	a = 4.9651 ± 0.0025 Å, c = 6.9263 ± 0.0021 Å	-	a = 7.7453 ± 0.0015 Å, b = 7.6482 ± 0.0013 Å, c = 5.7981 ± 0.0012 Å	a = 4.7578 ± 0.0017 Å, c = 12.9292 ± 0.0014 Å
0.45	a = 7.7129 ± 0.0012 Å, c = 5957 ± 0.0015 Å	a = 4.9592 ± 0.0016 Å, c = 6.9263 ± 0.0012 Å	-	a = 7.5018 ± 0.0012 Å, b = 7.6633 ± 0.0016 Å, c = 5.7936 ± 0.0017 Å	a = 4.7391 ± 0.0015 Å, c = 12.9853 ± 0.0012 Å
0.50	a = 7.7446 ± 0.0013 Å, c = 5.6191 ± 0.0016 Å	a = 4.9737 ± 0.0023 Å, c = 5.9327 ± 0.0012 Å	-	a = 7.5311 ± 0.0015 Å, b = 7.7114 ± 0.0014 Å, c = 5.7845 ± 0.0019 Å	a = 4.7549 ± 0.0014 Å, c = 12.9799 ± 0.0012 Å

Table A1. *Cont.*

Concentration of Al_2O_3, M	Lattice Parameter, Å				
	Si_3N_4	SiO_2	(SiAl)(ON)	$Al_2(SiO_4)O$	Al_2O_3
0.55	a = 7.7431 ± 0.0016 Å, c = 5.6012 ± 0.0012 Å	a = 4.9629 ± 0.0013 Å, c = 6.9466 ± 0.0019 Å	-	a = 7.5223 ± 0.0012 Å, b = 7.7024 ± 0.0015 Å, c = 5.7823 ± 0.0013 Å	a = 4.7484 ± 0.0012 Å, c = 12.9851 ± 0.0016 Å
0.60	a = 7.7889 ± 0.0015 Å, c = 5.5893 ± 0.0017 Å	a = 4.9885 ± 0.0016 Å, c = 6.9317 ± 0.0014 Å	-	a = 7.5487 ± 0.0016 Å, b = 7.7054 ± 0.0012 Å, c = 5.7823 ± 0.0013 Å	a = 4.7727 ± 0.0014 Å, c = 12.9904 ± 0.0017 Å
0.65	a = 7.7828 ± 0.0014 Å, c = 5.6245 ± 0.0022 Å	a = 4.9807 ± 0.0024 Å, c = 6.9426 ± 0.0021 Å	-	a = 7.5605 ± 0.0015 Å, b = 7.6964 ± 0.0013 Å, c = 5.7799 ± 0.0017 Å	a = 4.7652 ± 0.0016 Å, c = 12.9853 ± 0.0013 Å
0.70	a = 7.7281 ± 0.0016 Å, c = 5.6377 ± 0.0021 Å	a = 4.9709 ± 0.0023 Å, c = 6.9454 ± 0.0021 Å	-	a = 7.5458 ± 0.0016 Å, b = 7.6904 ± 0.0012 Å, c = 5.7845 ± 0.0019 Å	a = 4.7559 ± 0.0017 Å, c = 12.9547 ± 0.0021 Å
0.75	-	-	-	a = 7.5252 ± 0.0015 Å, b = 7.7084 ± 0.0012 Å, c = 5.7709 ± 0.0014 Å	a = 4.7503 ± 0.0015 Å, c = 12.9699 ± 0.0013 Å
0.80	-	-	-	a = 7.5237 ± 0.0013 Å, b = 7.6977 ± 0.0015 Å, c = 5.7562 ± 0.0021 Å	a = 4.7652 ± 0.0018 Å, c = 13.0261 ± 0.0011 Å
0.85	-	-	-	a = 7.5252 ± 0.0017 Å, b = 7.6904 ± 0.0013 Å, c = 5.7777 ± 0.0012 Å	a = 4.7708 ± 0.0016 Å, c = 13.0107 ± 0.0013 Å
0.90	-	-	-	a = 7.5164 ± 0.0015 Å, b = 7.6994 ± 0.0012 Å, c = 5.7755 ± 0.0016 Å	a = 4.7484 ± 0.0015 Å, c = 12.9598 ± 0.0012 Å
0.95	-	-	-	a = 7.5047 ± 0.0013 Å, b = 7.6937 ± 0.0017 Å, c = 5.7981 ± 0.0012 Å	a = 4.7820 ± 0.0017 Å, c = 13.0260 ± 0.0024 Å
1	-	-	-	-	a = 4.7503 ± 0.0016 Å, c = 12.9751 ± 0.0014 Å

References

1. Zinkle, S.J.; Terrani, K.A.; Snead, L.L. Motivation for utilizing new high-performance advanced materials in nuclear energy systems. *Curr. Opin. Solid State Mater. Sci.* **2016**, *20*, 401–410. [CrossRef]
2. Allen, T.R.; Sridharan, K.; Tan, L.; Windes, W.E.; Cole, J.I.; Crawford, D.C.; Was, G.S. Materials challenges for generation IV nuclear energy systems. *Nucl. Technol.* **2008**, *162*, 342–357. [CrossRef]
3. Zhan, L.; Bo, Y.; Lin, T.; Fan, Z. Development and outlook of advanced nuclear energy technology. *Energy Strategy Rev.* **2021**, *34*, 100630. [CrossRef]
4. Asmolov, V.G.; Zagryazkin, V.N.; Isaev, I.F.; Semenov, I.M.; Vishnevskii, V.Y.; D'yakov, E.K.; Udalov, Y.P. Choice of buffer material for the containment trap for VVER-1000 core melt. *At. Energy* **2002**, *92*, 5–14. [CrossRef]
5. Landälv, L. *Physical Vapor Deposition and Thermal Stability of Hard Oxide Coatings*; Linköping University Electronic Press: Linköping, Switzerland, 2019; Volume 1985.
6. Börner, F.D.; Lippmann, W.; Hurtado, A. Laser-joined Al_2O_3 and ZrO_2 ceramics for high-temperature applications. *J. Nucl. Mater.* **2010**, *405*, 1–8. [CrossRef]
7. Gharieb, M.; Kenawy, S.H.; El-Bassyouni, G.T.; Hamzawy, E.M. Gamma ray and fast neutron shielding of ZrSiO4-Al2O3 ceramic refractor. *Part. Sci. Technol.* **2023**, *41*, 250–260. [CrossRef]
8. Van Gestel, T.; Sebold, D.; Hauler, F.; Meulenberg, W.A.; Buchkremer, H.P. Potentialities of microporous membranes for H2/CO2 separation in future fossil fuel power plants: Evaluation of SiO_2, ZrO_2, Y_2O_3–ZrO_2 and TiO_2–ZrO_2 sol–gel membranes. *J. Membr. Sci.* **2010**, *359*, 64–79. [CrossRef]
9. Zhang, Y.; Bai, X.M. Ceramic materials for nuclear energy applications. *JOM* **2019**, *71*, 4806–4807. [CrossRef]
10. Sauder, C. Ceramic matrix composites: Nuclear applications. In *Ceramic Matrix Composites: Materials, Modeling and Technology*; John Wiley & Sons, Inc.: Hoboken, NJ, USA, 2014; pp. 609–646.
11. Ren, B.; Wang, Y.; Liu, J.; Zhang, X.; Chen, Y.; Rong, Y.; Yang, J. Preparation of Al_2O_3-Si_3N_4 porous ceramics with a cactus-like architecture for potential filters applications. *Ceram. Int.* **2019**, *45*, 6581–6584. [CrossRef]

12. Wang, C.; Wang, E.; Chen, J.; Chou, K.C.; Hou, X. The morphological evolution of the oxide products of Si_3N_4/Al_2O_3 composite refractory under different oxidizing conditions. *J. Ceram. Soc. Jpn.* **2017**, *125*, 661–669. [CrossRef]
13. Hayashi, K.; Onomura, Y. Effects of Annealing on Properties of Si_3N_4-MgO-Al_2O_3 Ceramics. *J. Jpn. Soc. Powder Powder Metall.* **1985**, *32*, 282–285. [CrossRef]
14. Izhevskiy, V.A.; Genova, L.A.; Bressiani, J.C.; Aldinger, F. Progress in SiAlON ceramics. *J. Eur. Ceram. Soc.* **2000**, *20*, 2275–2295. [CrossRef]
15. Celik, A.; Lazoglu, I.; Kara, A.; Kara, F. Investigation on the performance of SiAlON ceramic drills on aerospace grade CFRP composites. *J. Mater. Process. Technol.* **2015**, *223*, 39–47. [CrossRef]
16. Liu, G.; Chen, K.; Li, J. Combustion synthesis of SiAlON ceramic powders: A review. *Mater. Manuf. Process.* **2013**, *28*, 113–125. [CrossRef]
17. Galusek, D.; Ghillányová, K. Ceramic oxides. *Ceram. Sci. Technol.* **2010**, *2*, 4.
18. Singh, K.; Kaur, M.; Kumar, A. Progress in advanced ceramics: Energy and environmental perspective. In *Advanced Ceramics for Energy and Environmental Applications*; CRC Press: Boca Raton, FL, USA, 2021; pp. 1–12.
19. Dal Col, U. Joining of Porous Alloys by Glass Ceramics for Energy Applications. Ph.D. Thesis, Politecnico di Torino, Torino, Italy, 2021.
20. Besisa, D.H.; Ewais, E.M. Advances in functionally graded ceramics–processing, sintering properties and applications. In *Advances in Functionally Graded Materials and Structures*; InTech: Rijeka, Croatia, 2016; Volume 1, pp. 1–3.
21. Keane, M.A. Ceramics for catalysis. *J. Mater. Sci.* **2003**, *38*, 4661–4675. [CrossRef]
22. Borgekov, D.B.; Kozlovskiy, A.L.; Zdorovets, M.V.; Shakirzyanov, R.I.; Kenzhina, I.E.; Shlimas, D.I. Synthesis and Characterization of the Properties of (1−x) Si_3N_4-xAl_2O_3 Ceramics with Variation of the Components. *Materials* **2023**, *16*, 1961. [CrossRef] [PubMed]
23. El-Amir, A.A.; El-Maddah, A.A.; Ewais, E.M.; El-Sheikh, S.M.; Bayoumi, I.M.; Ahmed, Y.M.Z. Sialon from synthesis to applications: An overview. *J. Asian Ceram. Soc.* **2021**, *9*, 1390–1418. [CrossRef]
24. Cai, J.; Zhang, Y.L.; Li, Y.; Du, L.Y.; Lyu, Z.Y.; Wu, Q.; Hu, Z. Synthesis of three-dimensional AlN–Si 3 N 4 branched heterostructures and their photoluminescence properties. *CrystEngComm* **2014**, *16*, 9555–9559. [CrossRef]
25. Zanocco, M.; Marin, E.; Boschetto, F.; Adachi, T.; Yamamoto, T.; Kanamura, N.; Pezzotti, G. Surface functionalization of polyethylene by silicon nitride laser cladding. *Appl. Sci.* **2020**, *10*, 2612. [CrossRef]
26. Neuville, D.R.; Charpentier, T.; Du, J.C.; Yue, Y.Z.; Blanc, W.; Cicconi, M.R.; Yue, Y. Structure characterizations and molecular dynamics simulations of melt, glass, and glass fibers. In *Fiberglass Science and Technology: Chemistry, Characterization, Processing, Modeling, Application, and Sustainability*; Springer International Publishing: Cham, Switzerland, 2021; pp. 89–216.
27. Vural, S.; Sari, Ö. Synthesis and characterization of SDS assistant α-alumina structures and investigation of the effect of the calcination time on the morphology. *Colloid Polym. Sci.* **2019**, *297*, 107–114. [CrossRef]
28. Dwivedi, S.P. Effect of microwave sintering on the microstructure and mechanical properties of Al-Al_2O_3-Si_3N_4 hybrid composite fabricated by powder metallurgy techniques. *Proc. Inst. Mech. Eng. Part C J. Mech. Eng. Sci.* **2023**, *237*, 5052–5065. [CrossRef]
29. Hao, S.M.; Wang, H.F. Effect of Nano-Al_2O_3 on Mechanical Properties and Microstructure of Al_2O_3/Si_3N_4 Compound Ceramics. *Adv. Mater. Res.* **2011**, *168*, 1846–1849.
30. Wang, H.F.; Hao, S.M.; Bi, Y.B.; Yu, R.H. Effect of nanosized Al_2O_3 as additive on the sintering characteristics and vickers hardness of Al_2O_3/Si_3N_4 compound ceramics. *Adv. Mater. Res.* **2011**, *214*, 178–181. [CrossRef]
31. Li, X.L.; Chen, X.L.; Ji, H.M.; Sun, X.H.; Zhao, L.G. Phase analysis and thermal conductivity of in situ O′-sialon/β-Si_3N_4 composites. *Int. J. Miner. Metall. Mater.* **2012**, *19*, 757–761. [CrossRef]
32. Zha, J.W.; Dang, Z.M.; Li, W.K.; Zhu, Y.H.; Chen, G. Effect of micro-Si_3N_4-nano-Al_2O_3 co-filled particles on thermal conductivity, dielectric and mechanical properties of silicone rubber composites. *IEEE Trans. Dielectr. Electr. Insul.* **2014**, *21*, 1989–1996. [CrossRef]
33. Yang, R.; Xu, J.; Guo, J.; Meng, X.; Zhang, P.; Fan, F.; Gao, F. High wave transmittance and low thermal conductivity γ-α-SiAlON porous ceramics for high-temperature radome applications. *J. Adv. Ceram.* **2023**, *12*, 1273–1287. [CrossRef]
34. Kitayama, M.; Hirao, K.; Toriyama, M.; Kanzaki, S. Thermal conductivity of ß-Si_3N_4: I, effects of various microstructural factors. *J. Am. Ceram. Soc.* **1999**, *82*, 3105–3112. [CrossRef]
35. Kaidash, O.N.; Fesenko, I.P.; Kryl, Y.A. Heat conductivity, physico-mechanical properties and interrelations of them and structures of pressureless sintered composites produced of Si_3N_4-Al_2O_3-Y_2O_3 (-ZrO_2) nanodispersed system. *J. Superhard Mater.* **2014**, *36*, 96–104. [CrossRef]
36. Deng, Z.Y.; Ferreira, J.M.; Tanaka, Y.; Isoda, Y. Microstructure and thermal conductivity of porous ZrO_2 ceramics. *Acta Mater.* **2007**, *55*, 3663–3669. [CrossRef]
37. Hostaša, J.; Pabst, W.; Matějíček, J. Thermal conductivity of Al_2O_3–ZrO_2 composite ceramics. *J. Am. Ceram. Soc.* **2011**, *94*, 4404–4409. [CrossRef]
38. Guo, J.; Xu, J.; Yang, R.; Chen, K.; Yan, H.; Gao, F. Effect of composition on the dielectric properties and thermal conductivity of α-SiAlON ceramics. *J. Mater. Sci. Mater. Electron.* **2022**, *33*, 22480–22491. [CrossRef]

39. Xie, L.; Yao, D.; Xia, Y.; Yin, J.; Liang, H.; Zuo, K.; Zeng, Y. High porosity Ca-α-SiAlON ceramics with rod-like grains fabricated by freeze casting and pressureless sintering. *J. Eur. Ceram. Soc.* **2019**, *39*, 2036–2041. [CrossRef]
40. Lee, C.S.; Lemberg, J.A.; Cho, D.G.; Roh, J.Y.; Ritchie, R.O. Mechanical properties of Si_3N_4–Al_2O_3 FGM joints with 15 layers for high-temperature applications. *J. Eur. Ceram. Soc.* **2010**, *30*, 1743–1749. [CrossRef]